Simulating the effects of side-aspect fish orientation on acoustic biomass estimates

Kevin M. Boswell, Brian M. Roth, and James H. Cowan, Jr

Simulation methods were used to investigate the effect of side-aspect fish orientation on estimates of fish biomass derived from acoustic data. Three population-level length distributions ($n = 1000$ individuals) were simulated (identical, uniform, and age class) and applied to a target strength (TS) function of fish length previously derived for Gulf menhaden (*Brevoortia patronus*). Systematic manipulation of the TS–length coefficients strongly affected the biomass estimates. Based on simulations, biomass estimates decreased markedly from the true side-aspect to head- or tail-on orientation, with estimates of population biomass decreasing by 80% when orientation deviated by as little as 30° from true side-aspect. Simulated data indicate that biomass estimates generated from surveys may be grossly inaccurate if fish orientation is not taken into account.

K. M. Boswell and J. H. Cowan, Jr: Department of Oceanography and Coastal Sciences, School of the Coast and Environment, Louisiana State University, Baton Rouge, LA 70803, USA. B. M. Roth: Department of Fisheries and Wildlife, Michigan State University, 13 Natural Resources Building, East Lansing, MI 48824, USA. Correspondence to K. M. Boswell: tel: +1 225 578 9390; fax: +1 225 578 6513; e-mail: kboswe1@lsu.edu.

Introduction

For fishery surveys to serve as useful indices of biological benchmarks (e.g. biomass, density, abundance), attempts should be made to identify and quantify the sources of uncertainty (Rose et al., 2000) so decreasing survey error. Acoustic surveys, often considered less biased than traditional fishing-based methods (e.g. trawls, traps, etc.), can be fraught with uncertainties from both systematic and random errors, see Simmonds and MacLennan (2005), with potential to mask the true survey results and conclusions. Nevertheless, acoustic surveys are often used to estimate the distribution of biological targets for assessment purposes (Demer and Conti, 2005; Mello and Rose, 2005; Simmonds and MacLennan, 2005; Løland et al., 2007; Walline, 2007). Common sources of error include measurement error (Rose et al., 2000), target strength (TS) variability (Demer, 2004; Demer and Conti, 2005); calibration error (Rose et al., 2000); environmental noise (Simmonds and MacLennan, 2005); and behavioural variability (Kubecka and Duncan, 1998; Drastik and Kubecka, 2004; Løland et al., 2007). However, TS appears to have the greatest potential to bias survey results (Simmonds and MacLennan, 2005).

It is well understood that fish orientation and condition can significantly affect the scattering intensity observed from a fish (Love, 1977; Foote, 1980; McClatchie et al., 1996; Ona, 2003). When using a vertically aimed transducer, changes in the fish tilt-angle can produce marked changes in measured TS (Foote, 1980; McClatchie et al., 1996; Benoit-Bird and Au, 2001); changes in the TS measured at side-aspects can be even more pronounced (Kubecka and Duncan, 1998; Lilja et al., 2000; Frouzova et al., 2005; Boswell and Wilson, 2008). Large variations in the

measured scattering strength will inevitably lead to uncertainty and error in the biomass estimates of a surveyed population (Rose et al., 2000).

Side-aspect acoustic surveys are becoming common in shallow-water areas where the more traditional vertical-sounding methods are impractical (Kubecka and Wittinegerova, 1998; Pedersen and Trevorrow, 1999; Boswell and Wilson, 2008). However, researchers are more likely to encounter unpredictable changes in TS estimates for schooling fish, given their polarized swimming behaviour. Consequently, these changes in fish behaviour may ultimately translate into unexplained variability in the biomass estimates for schooling fish.

In this paper, we demonstrate how three sources of variation could affect the acoustic estimates of fish biomass for a schooling species. Our objectives were to quantify the effect of (i) the length–weight relationship, (ii) fish orientation, and (iii) TS–length regression coefficients on the estimates of fish biomass. The goal was to identify how these sources of error could affect the estimates of biomass calculated using acoustic data. There are many sources of uncertainty in fishery acoustics, and their relative contributions to uncertainty in empirically determined biomass estimates require better evaluation.

Methods

To identify the relative magnitude of the error associated with each factor cited, three populations (each with $n = 1000$) were simulated. The first, comprising only 7 cm individuals, is hereafter called the "identical" population. The second had a mean length of 7 cm, but comprised individuals whose lengths were taken from a uniform random distribution between 3.5 and 10.5 cm

(i.e. mean length $\pm 50\%$), hereafter referred to as the "uniform" population. The third was a simulated population comprising three age classes, where the youngest (age 0) had a mean length of 3 cm, the second youngest (age 1) a mean length of 7 cm, and the oldest (age 2) a mean length of 10 cm (Figure 1). A random normal distribution of lengths within each age class was assumed, so that the standard deviation (s.d.) around the mean was 0.5 cm for age-0 fish, 0.75 cm for age-1 fish, and 1.0 cm for age-2 fish. This simulated population is hereafter called the "age-class" population.

For each analysis, except that of the length–weight equation, the "true" side-aspect *TS* response (TS_{true}, dB re 1 m^2) was simulated based on the TS–length function derived for Gulf menhaden (*Brevoortia patronus*), a dominant fish in northern Gulf of Mexico estuaries (Rozas and Reed, 1994; Rozas and Zimmerman, 2000; Jones et al., 2002):

$$TS_{\text{true}} = a \log_{10}(L) + b, \qquad (1)$$

where the nominal values for a and b are 26.1 and -65.6, respectively, and the fish length L is in centimetres (Boswell and Wilson, 2008). Changes in fish orientation (θ, in degrees) relative to the lateral axis of the target were calculated as deviations on TS_{true}. In general, TS has a parabolic relationship with orientation as a fish rotates from $0°$ (side-aspect) to $90°$ (head- or tail-on perspective; Love, 1977; Kubecka and Duncan, 1998; Boswell and Wilson, 2008). The parabolic fit to the TS distributions from Gulf menhaden is

$$TS_{\theta} = 0.0013(\theta)^2 + 0.2354(\theta) - 42.65, \qquad (2)$$

where TS_{θ} is the TS of a fish at angle θ relative to the side-aspect. TS_{θ} was normalized to a maximum of 1 at $0°$ to determine the proportional deviation (γ) in TS caused by changes in orientation relative to the side-aspect:

$$\gamma = -0.00003(\theta)^2 + 0.0054(\theta) + 1. \qquad (3)$$

It was assumed that the proportional deviation was independent of fish size. Thus, the TS derived through the simulation is the product of TS_{true} and γ and represents the actual TS (TS_{ACT}):

$$TS_{\text{ACT}} = TS_{\text{true}} \times \gamma. \qquad (4)$$
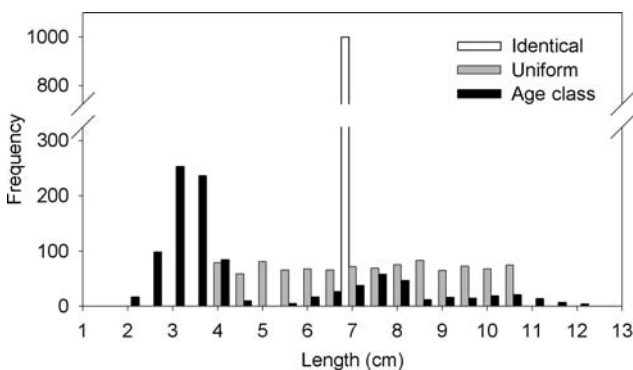
Figure 1. Length frequency distributions of the three populations: identical, uniform, and age class. For each population, $n = 1000$ individuals.

Consequently, fish lengths (L, cm) calculated using the deviation from side-aspect ($\theta = 0$) were

$$L = 10^{(TS_{\text{ACT}} - b)/a}, \qquad (5)$$

where the nominal values of a and b as stated above were used. Thus, when $\theta = 0^0$, $TS_{\text{ACT}} = TS_{\text{true}}$. Fish mass (g) was calculated using the length–weight equation for menhaden proposed by Vaughan et al. (2000):

$$\text{mass(g)} = 0.0119\, L^{3.2}. \qquad (6)$$

The biomass for each population was determined by summing across all individuals within each population. For all analyses, population biomass was standardized to the value calculated with the nominal equation coefficients. Standardizing the response allows at least a qualitative judgement of how each treatment affects the biomass calculations. Wherever possible, the independent variables were also standardized to determine how proportional changes in the nominal equation coefficients affected the biomass estimate.

Length–weight equation error

The effect of error in Equation (6) on the biomass of each population was determined. Gaussian noise was added to the exponent in Equation (6), with a mean of zero and s.d. = 0.0, 0.05, 0.10, 0.15, 0.20, and 0.25. Adding this noise caused increasing deviations from the simulated mean weight for a given length. The analysis was limited to s.d. values of ≤ 0.25 to constrain the estimates of weight-at-length within reasonable bounds. For each population, 1000 numbers were drawn from the Gaussian distribution, that is to say, the number of individuals in each population. This value was added to the exponent before calculating the weight for each length.

Fish-orientation error

Two separate analyses were conducted to investigate how fish orientation affects biomass estimates. The first determined the population biomass for fish that were all orientated in the same direction, where the biomass was calculated at $5°$ orientation increments between 0 and $90°$. It was assumed that fish orientated at $\theta < 0°$ or $>90°$ would provide mirror-image TS variations over adjacent angles. For example, according to Equation (4), fish orientated at $\theta = 82°$ and $98°$ should have the same TS_{ACT}, and likewise for fish orientated at $\theta = 295°$ ($-5°$) and $+5°$. To isolate the effect of orientation error, the nominal values of the coefficients in Equation (5) were assumed.

For the second analysis, variability was introduced in the orientation of each fish within a given population at each $5°$ increment. Schooling fish are unlikely to orientate in one direction; some will be at angles greater or less than the population mean. To account for this, two types of variability were incorporated, by adding either random Gaussian (0, s.d.) or uniform (-0.5, 0.5) noise to the mean orientation of each fish. The selection of Gaussian and uniform distributions was an arbitrary choice to demonstrate how alternative distributions could affect biomass estimates. The magnitude of the noise was determined by a multiplier (k) applied to the s.d. of the Gaussian distribution (s.d. $\times k$) or to the limits of the uniform distribution ($-0.5\,k$ to $+0.5\,k$). Multipliers ranging from 0 to 10, at increments of 0.5, were applied to both the Gaussian and uniform noise distributions.
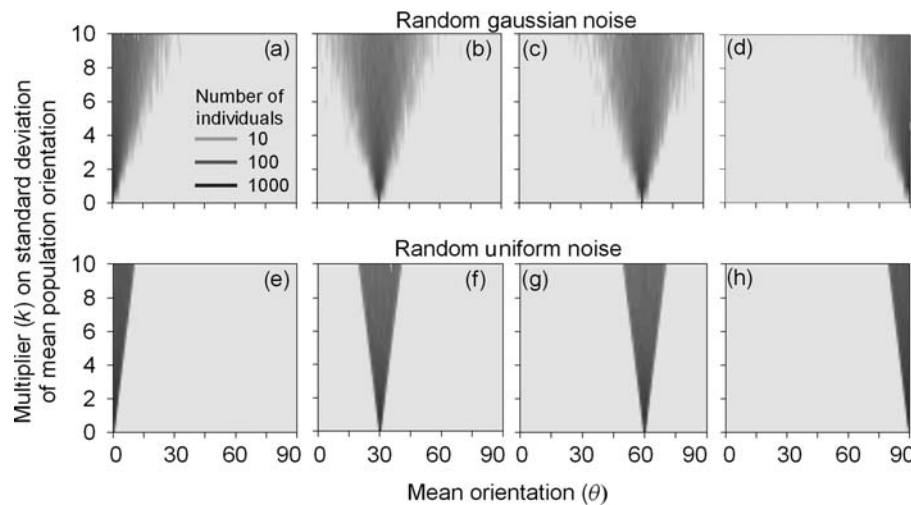
Figure 2. The effect of increasing variation in individual orientation within a population (*y*-axis) for mean orientations of (a) 0°, (b) 30°, (c) 60°, and (d) 90°. The multiplier (*k*) was applied to the s.d. of the Gaussian (s.d. × *k*) or the limits of the uniform ($-0.5 \times k$, $0.5 \times k$) distribution.

Increasing noise caused the orientation distributions within a population to spread either normally (Figure 2a–d) or uniformly around the mean value of θ (Figure 2e–h). The biomass of each population was calculated using the *TS* derived from Equation (4), accounting for individual orientation. By plotting the total fish biomass of each population against the range of multipliers at mean orientations (θ) of 0, 30, 60, and 90°, the effects of both normal- and uniform-orientation noise could be determined. Although biomass was calculated at every 5° increment, the four selected values of θ were suitably representative of trends that emerged during the analysis. The response (biomass) was standardized to 1, based on the "true" biomass for each population (determined at $\theta = 0°$ and s.d. = 0).

TS – length equation error

A systematic approach was used to quantify how variation in the *TS*–*L* function [Equation (1)] could affect population biomass estimates. *TS* values calculated using the original length distributions of each population (with $\theta = 0°$ and no orientation noise) were used to manipulate the *TS*–*L* coefficients in Equation (1). Here, *a* and *b* were manipulated systematically and used to recalculate fish lengths with Equation (5). At first glance, this may seem circular; however, the *TS* derived from the original length distributions was considered to be an arbitrary starting point for analysis. The *TS*–*L* coefficients in Equation (5) were varied $\pm 10\%$ in 1% increments to produce lengths that were converted to mass using the nominal coefficient values from Equation (6). A response surface was generated, relating total biomass for each population to the unique combinations of *a* and *b*. Response surfaces were produced for both actual and standardized coefficient values.

Results
Effect of length – weight equation error

For the three populations, adding more variability into the length–weight equation led to predictable alterations of the length–weight relationship. However, increasing variability had little effect on the estimates of the total biomass of each population (Table 1). Without error in the length–weight equation, the

Table 1. Biomass (g) values of the three populations calculated at increasing levels of variability (s.d.) imposed on the exponent of the length–weight equation.
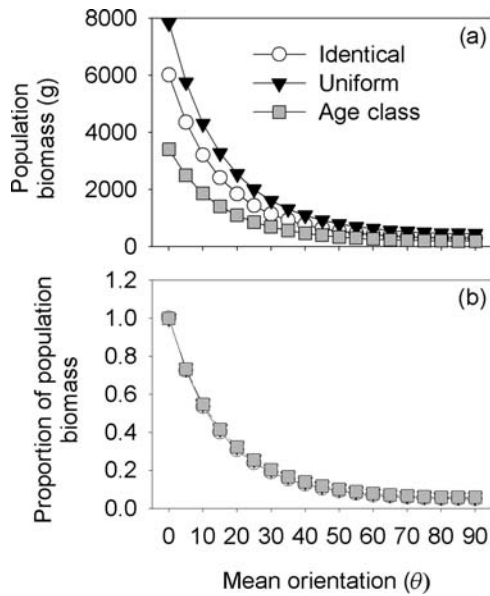
	Population		
s.d.	Identical	Uniform	Age class
0.00	6 023.7	7 840.1	3 408.1
0.05	6 052.0	7 857.7	3 392.8
0.10	6 130.4	7 986.0	3 500.8
0.15	6 375.7	8 298.2	3 531.7
0.20	6 531.4	8 439.0	3 806.4
0.25	6 851.2	8 708.6	3 779.6

biomass of the identical population was 6023 g. The biomasses of the uniform and age-class populations were 7840 and 3408 g, respectively. Compared with these baselines, the level of variability applied (s.d. = 0.25) produced population biomass estimates that increased by 14% (6851 g) for the identical population, 11% (8709 g) for the uniform population, and 11% (3781 g) for the age-class population.
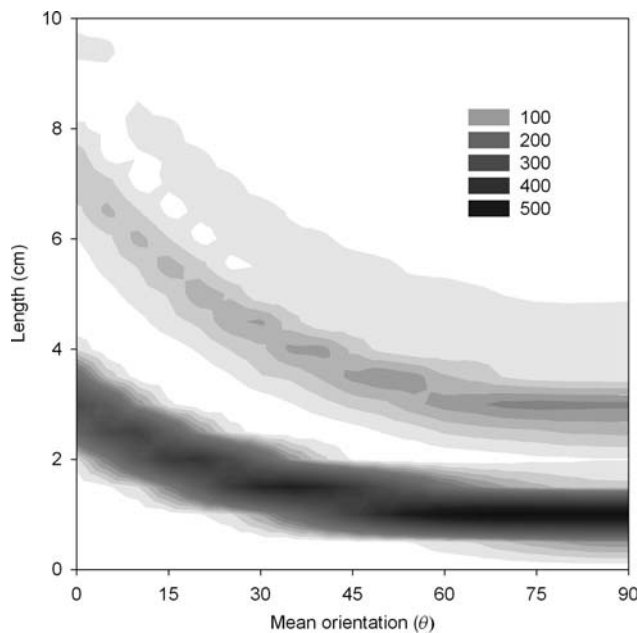
Effect of orientation on population biomass

Increasing θ away from 0° resulted in a large negative effect on the biomass estimates, which for all three populations declined exponentially with increasing angles of orientation (Figure 3). Consequently, orientations close to, but deviating away from $\theta = 0°$, resulted in strong negative bias in the biomass estimates. For instance, populations that were orientated at only $\theta = 5°$ produced biomass estimates 30% lower than the true values, and at $\theta = 10°$, the estimates were 50% lower (Figure 3b). Orientations more than $\theta = 10°$ resulted in severely biased estimates. At $\theta = 90°$, the estimated biomass for all three populations was only 5% of the true biomass. By increasing θ from 0°, a concomitant reduction in *TS* was observed, and this led to a narrower length frequency distribution (Figure 4).

In general, the mean orientation assigned to the population was the dominant determinant of biomass. Adding variation to a population's mean orientation had little influence on overall
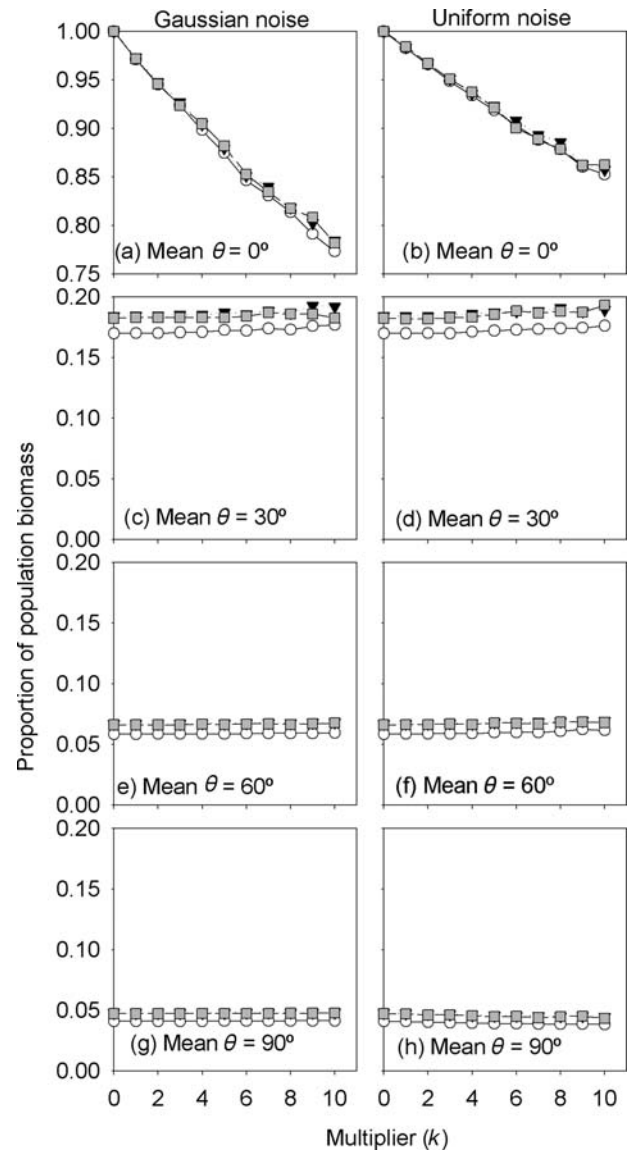
Figure 3. Relationship between fish orientation and estimated biomass for each population displayed as (a) total biomass and (b) proportion of true biomass. The nominal condition for (b) is defined as the biomass at $\theta = 0°$.

Figure 4. The effect of fish orientation (θ) on the estimated length frequency distribution for the age-class population. The nominal length frequency distribution occurs at $\theta = 0°$.

Figure 5. Effect of increasing the variation (k) of individual fish orientation (θ) on the proportional estimates of population biomass. Two types of variation were applied: random Gaussian (left) and random uniform (right). All three populations are illustrated: identical (triangle), uniform (circle), and age class (square).

biomass, excepting for mean $\theta = 0°$ (Figure 5). At $\theta = 0°$, increasing the Gaussian and uniform noise also resulted in negative bias, reducing the biomass estimate by 22% and 15%, respectively. Paralleling the first orientation analysis, values of $\theta > 0°$ reduced the biomass estimates (Figure 5c–h). At $\theta = 30°$, biomass increased slightly with increasing noise for each population, but remained between 18 and 20% of the true biomass always (Figure 5c and d). Both increasing and changing the nature of

noise had little effect on biomass estimates at $\theta = 60$ and $90°$, and all populations remained within 6 and 5% of the true biomass, respectively, at these orientations (Figure 5e–h).

Effect of error in the *TS*–length function

Systematic manipulation revealed that both coefficients in the *TS*–length function have a strong effect on biomass estimates. Estimated biomass consistently increased with larger *a* or *b*. This created isoclines that shifted linearly from left to right, moving up the *y*-axis with increasing values of *b* (Figure 6, only the age-class population is illustrated). Within the array of coefficients tested, biomass estimates ranged between 507 and 71 500 g for the identical population, between 625 and 98 800 g for the uniform population, and between 276 and 42 500 g for the age-class population. These ranges corresponded to an 11-fold
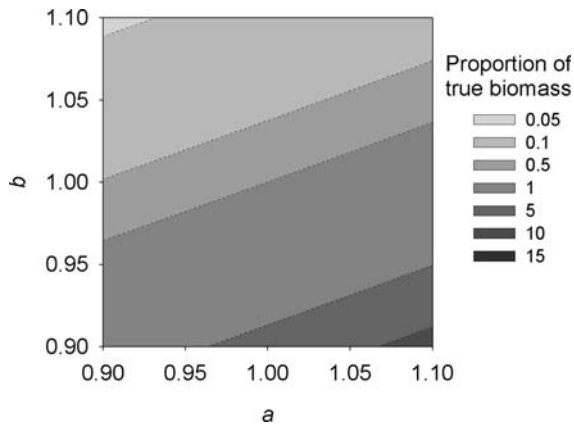
Figure 6. The effect of varying the $TS-L$ coefficients (a and b) on the standardized biomass of the age-class population. The biomass corresponding to the nominal coefficients lies in the centre of the plot at the point (1.0, 1.0). Plots for the other two populations were similar.
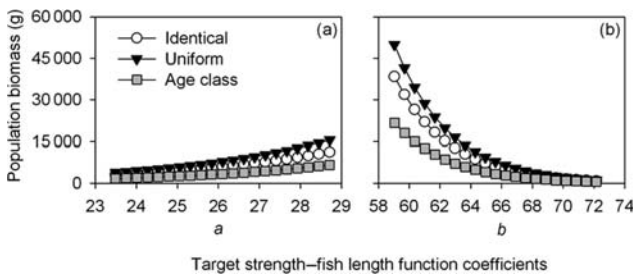
Figure 7. Cross sections of Figure 6 taken at the nominal value of a (panel a; 26.1) and b (panel b; −65.6) for each population.

change in biomass relative to the 10% increase or decrease in both a and b (Figure 6). The smallest biomass estimates corresponded to the lowest values of both a (23.5) and b (−72.2 dB; upper left-hand corner of Figure 6). Similarly, the greatest biomass corresponded to the largest value of both a (28.7) and b (−59.0 dB), that is to say, near the lower-right corner of Figure 6.

Cross sections of biomass vs. the TS−length coefficients revealed that proportional changes in a (Figure 7a) at the nominal value of b (−65.6 dB) have a lesser effect on biomass when compared with the same proportional changes in b (Figure 7b) at the nominal value of a (26.1). The biomass of the age-class population was ∼22 000 g at the greatest value of b, and <600 g at the lowest value of a. In contrast, the same population had a biomass of 1800 g at the lowest value of a, and ∼6600 g at the highest value of a. These patterns were similar for the other two populations, although the absolute values were greater (Figure 7).

Discussion

In this series of simulations, three different, population-level, fish length distributions were generated to provide discernible contrast in calculated biomass estimates as a function of fish orientation for schooling species. Although it is unlikely that a real fish population would resemble the "identical" case, inclusion of that distribution served as a baseline for comparison with the other distributions. The uniform and age-class distributions are commonly used in

modelling studies to predict size-based characteristics of fish populations. The age-class model most closely resembles the size distributions of a natural population and serves as the likely candidate to compare with natural systems. However, *in situ* observation is the most appropriate method to determine the proper length frequency distribution to describe a given population.

Biomass estimates generated from acoustic surveys are generally, though tenuously, regarded as relative estimates (Yule, 2000; Boswell *et al.*, 2007). Based on the simulations reported here, indices of biomass can be considered useful and interpretable when accounting for *in situ* orientation. The results indicate that the two most important sources of error are the $TS-L$ coefficients (a and b) and the ability to account for fish orientation. Slight deviations in the coefficients generated measurable effects on biomass estimates. Most notably, the intercept (b) elicited large proportional changes in biomass estimates. This result is consistent with that of Boswell *et al.* (2008a), who applied five different $TS-L$ functions to field data and demonstrated that the choice of coefficients can result in disparate biomass estimates.

Changes in orientation away from the side-aspect ($\theta = 0°$) led to substantial declines in the observed biomass estimates. As the fish orientation changed from $\theta = 0$ to $30°$, the population biomass predicted by the presented models decreased by 80% of the simulated "true" value. Therefore, as the apparent cross section of the swimbladder changed with the fish orientation, the predicted biomass estimates decreased sharply, specifically within the first $30°$ from $\theta = 0°$.

Although we analysed each source of error individually, the potential bias from both an imprecise $TS-L$ function and the unknown orientation of the insonified fish suggests a significant cumulative effect on the estimates of population biomass. Although it is possible to minimize this effect by accounting for orientation based upon direct observation, for example, with video or imaging sonars such as the DIDSON, most surveys are not yet designed to accommodate such ground-truthing. In addition to error associated with the uncertain orientation, the doubtful identification and partitioning of scattering data by different taxa has also been reported as a significant source of error (Rose *et al.*, 2000; Simmonds and MacLennan, 2005) and that problem requires further evaluation.

As demonstrated through these simulations, perhaps the simplest criterion for reducing error is assuming a single-species assemblage, with a mean population-level orientation. Except for targets orientated at a mean $\theta = 0°$, the TS estimates do not change significantly with the variation in population orientation. For example, if the mean orientation is $\theta = 30°$, the increase in the variation of individual orientations within the population does not appear to affect estimates of the population biomass significantly. Therefore, if a $TS-L$ function that accounted for mean population orientation could be applied, it might be feasible to correct the overall estimates of population biomass accordingly. Of course, this might not be feasible when there are multispecies assemblages present, with different scattering strengths among species (McClatchie *et al.*, 1996). Moreover, the proposed methods would likely be unrepresentative of non-schooling fish whose swimming behaviour could be better represented as random. When applying a random component to the three modelled populations, such that the orientation of each individual within each population is assumed randomly distributed between $\theta = 0$ and $90°$, the population estimates were reduced by 82–84% relative to the "true" values, as illustrated in row 1 of Table 1.

To reduce the uncertainty in a given survey, every effort should be made to eliminate or diminish the magnitude of known error sources. When considering fish orientation, perhaps the most plausible method is to acquire *in situ* information on the orientation and behaviour of targets simultaneously, in addition to the routine acoustic data collected during surveys. The DIDSON imaging sonar was recently used in field studies to acquire data on the *in situ* size, behaviour, density, and orientation of targets within an insonified volume (Moursund *et al.*, 2003; Holmes *et al.*, 2006; Burwen *et al.*, 2007; Boswell *et al.*, 2008b). In some cases, such information could facilitate the proper classification of acoustic targets on a taxon-specific level (Burwen *et al.*, 2007). This could contribute to an overall reduction in survey error, as described by Rose *et al.* (2000). Though simulation exercises are useful, they are limited by the quality of the initial parameter values. It is suggested that before undertaking extensive acoustic surveys, the sources of uncertainty that contribute to error should be identified and a plan should be developed to mitigate them. In addition, to reduce the overall survey error, the simultaneous application of novel techniques to ground-truth the assumed property of insonified targets is to be encouraged.

References

Benoit-Bird, K. J., and Au, W. W. L. 2001. Target strength measurements of Hawaiian mesopelagic boundary community animals. Journal of the Acoustical Society of America, 110: 812–819.

Boswell, K. M., Kaller, M. D., Cowan, J. H., and Wilson, C. A. 2008a. Evaluation of target strength-fish length equation choices for estimating estuarine fish biomass. Hydrobiologia, 610: 113–123.

Boswell, K. M., and Wilson, C. A. 2008. Side-aspect target-strength measurements of bay anchovy (*Anchoa mitchilli*) and Gulf menhaden (*Brevoortia patronus*) derived from *ex situ* experiments. ICES Journal of Marine Science, 65: 1012–1020.

Boswell, K. M., Wilson, M. P., and Cowan, J. H. 2008b. A semiautomated approach to estimating fish size, abundance, and behavior from dual-frequency identification sonar (DIDSON). North American Journal of Fisheries Management, 28: 799–807.

Boswell, K. M., Wilson, M. P., and Wilson, C. A. 2007. Hydroacoustics as a tool for assessing fish biomass and size distribution associated with discrete shallow water estuarine habitats in Louisiana. Estuaries and Coasts, 30: 607–617.

Burwen, D. L., Fleischman, S. J., and Miller, J. D. 2007. Evaluation of a dual-frequency imaging sonar for estimating fish size in the Kenai River. Alaska Department of Fish and Game, Fishery Data Series 07-44, Anchorage.

Demer, D. A. 2004. An estimate of error for the CCAMLR 2000 survey estimate of krill biomass. Deep Sea Research II, 51: 1237–1251.

Demer, D. A., and Conti, S. G. 2005. New target-strength model indicates more krill in the Southern Ocean. ICES Journal of Marine Science, 62: 25–32.

Drastik, V., and Kubecka, J. 2004. Fish avoidance of acoustic survey boat in shallow waters. Fisheries Research, 72: 219–228.

Foote, K. G. 1980. Effect of fish behaviour on echo energy: the need for measurements of orientation distributions. Journal du Conseil International pour l'Exploration de la Mer, 39: 193–201.

Frouzova, J., Kubecka, J., Balk, H., and Frouz, J. 2005. Target strength of some European fish species and its dependence on fish body parameters. Fisheries Research, 75: 86–96.

Holmes, J. A., Cronkite, G. M. W., Enzenhofer, H. J., and Mulligan, T. J. 2006. Accuracy and precision of fish-count data from a

"dual-frequency identification sonar" (DIDSON) imaging system. ICES Journal of Marine Science, 63: 543–555.

Jones, R. F., Baltz, D. M., and Allen, R. L. 2002. Patterns of resource use by fishes and macroinvertebrates in Barataria Bay, Louisiana. Marine Ecology Progress Series, 237: 271–289.

Kubecka, J., and Duncan, A. 1998. Acoustic size vs. real size relationships for common species of riverine fish. Fisheries Research, 35: 115–125.

Kubecka, J., and Wittingerova, M. 1998. Horizontal beaming as a crucial component of acoustic fish stock assessment in freshwater reservoirs. Fisheries Research, 35: 99–106.

Lilja, J., Marjomäki, T. J., Riikonen, R., and Jurvelius, J. 2000. Side-aspect target strength of Atlantic salmon (*Salmo salar*), brown trout (*Salmo trutta*), whitefish (*Coregonus lavaretus*), and pike (*Esox lucius*). Aquatic Living Resources, 13: 355–360.

Løland, A., Aldrin, M., Ona, E., Hjellvik, V., and Holst, J. C. 2007. Estimating and decomposing total uncertainty for survey-based abundance estimates of Norwegian spring-spawning herring. ICES Journal of Marine Science, 64: 1302–1312.

Love, R. H. 1977. Target strength of an individual fish at any aspect. Journal of the Acoustical Society of America, 62: 1397–1403.

McClatchie, S., Alsop, J., Ye, Z., and Coombs, R. F. 1996. Consequence of swimbladder model choice and fish orientation to target strength of three New Zealand fish species. ICES Journal of Marine Science, 53: 847–862.

Mello, L. G. S., and Rose, G. A. 2005. Using geostatistics to quantify seasonal distribution and aggregation patterns of fishes: an example of Atlantic cod (*Gadus morhua*). Canadian Journal of Fisheries and Aquatic Sciences, 62: 659–670.

Moursund, R. A., Carlson, T. J., and Peters, R. D. 2003. A fisheries application of a dual-frequency identification sonar acoustic camera. ICES Journal of Marine Science, 60: 678–683.

Ona, E. 2003. An expanded target-strength relationship for herring. ICES Journal of Marine Science, 60: 493–499.

Pedersen, B., and Trevorrow, M. V. 1999. Continuous monitoring of fish in a shallow channel using a fixed horizontal sonar. Journal of the Acoustical Society of America, 105: 3126–3135.

Rozas, L. P., and Reed, D. J. 1994. Comparing nekton assemblages of subtidal habitats in pipeline canals traversing brackish and saline marshes in coastal Louisiana. Wetlands, 14: 262–275.

Rozas, L. P., and Zimmerman, R. J. 2000. Small-scale pattern of nekton use among marsh and adjacent shallow non-vegetated areas of the Galveston Bay Estuary, Texas (USA). Marine Ecology Progress Series, 193: 217–239.

Rose, G. A., Gauthier, S., and Lawson, G. 2000. Acoustic surveys in the full monte: simulating uncertainty. Aquatic Living Resources, 13: 367–372.

Simmonds, E. J., and MacLennan, D. N. 2005. Fisheries Acoustics: Theory and Practice, 2nd edn. Blackwell Science, Oxford.

Vaughan, D. S., Smith, J. W., and Prager, M. H. 2000. Population characteristics of Gulf menhaden, *Brevoortia patronus*. NOAA Technical Report NMFS/149. 19 pp.

Walline, P. D. 2007. Geostatistical simulations of eastern Bering Sea walleye pollock spatial distributions, to estimate sampling precision. ICES Journal of Marine Science, 64: 559–569.

Yule, D. 2000. Comparison of horizontal acoustic and purse-seine estimates of salmonid densities and sizes in eleven Wyoming waters. North American Journal of Fisheries Management, 20: 759–775.